Developmental changes in P2X purinoceptors on glycinergic presynaptic nerve terminals projecting to rat substantia gelatinosa neurones

Il-Sung Jang, Jeong Seop Rhee, Hisahiko Kubota, Norihiko Akaike * and Norio Akaike

*Cellular and System Physiology, Graduate School of Medical Sciences, Kyushu University, Fukuoka 812-8582 and * Laboratory of Cellular Signaling, Faculty of Integrated Arts and Sciences, The University of Tokushima, Tokushima 770-8502, Japan*

1. In mechanically dissociated rat spinal cord substantia gelatinosa (SG) neurones attached with native presynaptic nerve endings, glycinergic miniature inhibitory postsynaptic currents (mIPSCs) were recorded using nystatin perforated patch recording mode under voltage-clamp conditions. Under these conditions, it was tested whether the changes in P2X receptor subtype on the glycinergic presynaptic nerve terminals occur during postnatal development.

2. ATP facilitated glycinergic mIPSC frequency in a concentration-dependent manner through all developmental stages tested, whereas $\alpha\beta$-methylene-ATP ($\alpha\beta$-me-ATP) was only effective at later developmental stages.

3. $\alpha\beta$-me-ATP-elicited mIPSC frequency facilitation was completely occluded in the Ca^{2+}-free external solution, but it was not affected by adding 10^{-4} M Cd^{2+}.

4. $\alpha\beta$-me-ATP still facilitated mIPSC frequency even in the presence of 10^{-6} M thapsigargin, a Ca^{2+} pump blocker.

5. In later developmental stages, ATP-elicited presynaptic or postsynaptic responses were reversibly blocked by 10^{-5} M pyridoxal-5-phosphate-6-azophenyl-2′,4′-disulfonic acid (PPADS), but only partially blocked by 10^{-7} M 2′,3′-*O*-(2,4,6-trinitrophenyl)-ATP (TNP-ATP). However, $\alpha\beta$-me-ATP-elicited presynaptic or postsynaptic responses were completely and reversibly blocked by either 10^{-5} M PPADS or 10^{-7} M TNP-ATP.

6. $\alpha\beta$-me-ATP significantly reduced the evoked glycinergic IPSC amplitude in postnatal 28–30 day neurones, whereas it had no effect in 10–12 day neurones.

7. It was concluded that $\alpha\beta$-me-ATP-sensitive P2X receptors were functionally expressed on the glycinergic presynaptic nerve terminals projecting to SG neurones in later developmental stages. Such developmental changes of presynaptic P2X receptor subtypes might contribute to synaptic plasticity such as the regulation of neuronal excitability and the fine controlling of the pain signal in spinal dorsal horn neurones.

P2X receptors activated by ATP are non-selectively permeable to cations, including Na^+, K^+ and Ca^{2+} (Chen *et al.* 1995; Buell *et al.* 1996; Taschenberger *et al.* 1999). Seven different P2X receptor subunit genes have been cloned from various tissues (Valera *et al.* 1994; Chen *et al.* 1995; Lewis *et al.* 1995; Buell *et al.* 1996; Collo *et al.* 1996; Garcia-Guzman *et al.* 1997; North & Barnard, 1997). Of these cloned receptors, the P2X1, P2X2, P2X3, P2X4, P2X5 and P2X6 subunits are expressed in the CNS (Collo *et al.* 1996; Vulchanova *et al.* 1996, 1998), and the P2X2, P2X4 and P2X6 subunits are also expressed in the

superficial laminae of the spinal cord dorsal horn (Collo *et al.* 1996; Vulchanova *et al.* 1997; Le *et al.* 1998*b*).

ATP acts as a fast excitatory neurotransmitter through the ionotropic P2X receptors in the superficial laminae of the dorsal horn (Edwards *et al.* 1992; Bardoni *et al.* 1997) and the peripheral nervous system (Evans *et al.* 1992; Galligan & Bertrand, 1994). ATP also acts as a neuromodulator through the presynaptic P2X receptors. For example, ATP modulates glutamate release from the nerve terminals of dorsal root ganglion (DRG) neurones

co-cultured with dorsal horn neurones (Gu & MacDermott, 1997). Li *et al.* (1998) also suggested that P2X2 receptors modulate excitatory synaptic transmission between primary afferent fibres and spinal dorsal horn neurones. Recently, Hugel & Schlichter (2000) reported that ATP, through P2X2 receptors, facilitates the GABAergic inhibitory transmission among cultured rat dorsal horn neurones. We have previously shown that ATP facilitates glycine release through P2X2 receptors in the dorsal horn lamina II neurones (Rhee *et al.* 2000). Thus, the P2X2 receptor on the inhibitory presynaptic nerve terminals has an important role in the negative feedback system, to protect against excessive excitation of substantia gelatinosa (SG) neurones in response to nociceptive input.

However, a question still remains as to whether other P2X receptors might act functionally on the modulation of neurotransmitter release in the dorsal horn of the spinal cord during postnatal development. In fact, most of the binding or immunohistochemical studies which demonstrated the existence of P2X2, P2X4 and P2X6 subunit RNAs in the dorsal horn have been conducted in adult rats (Collo *et al.* 1996; Vulchanova *et al.* 1996, 1997). Accordingly, in this study, we have investigated whether different kinds of P2X receptor subtypes appear during postnatal development using a synaptic bouton preparation (Rhee *et al.* 1999, 2000). This preparation allows us to focus selectively on the P2X receptor-mediated effects, because in slice preparation exogenously applied ATP is often hydrolysed to adenosine by extracellular nucleotidases (Dunwiddie *et al.* 1997).

METHODS

Mechanical dissociation

Wistar rats (10–30 days old) were decapitated under pentobarbital anaesthesia (50 mg kg^{-1}, I.P.). The lumbar enlargement of the spinal cord was quickly removed and transversely sliced at a thickness of 400 μm using a microslicer (VT1000S, Leica, Germany). Slices were kept in the control incubation medium (see below) saturated with 95% O_2 and 5% CO_2 at room temperature (22–24 °C) for at least 1 h. For dissociation, slices were transferred to a 35 mm culture dish (Primaria 3801, Becton Dickinson, NJ, USA) and the dorsal horn region of the spinal cord was identified under a binocular microscope (SMZ-1, Nikon, Tokyo, Japan). The details of mechanical dissociation have been described previously (Rhee *et al.* 1999, 2000). Briefly, mechanical dissociation was accomplished using a custom-built vibration device and a fire-polished glass pipette oscillating at about 3–5 Hz (0.1–0.2 mm). The tip of the fire-polished glass pipette was lightly placed on the surface of the dorsal horn region (layer II) with a micromanipulator. The tip of the glass pipette was vibrated horizontally for about 2 min. Slices were removed and the mechanically dissociated neurones allowed to settle and adhere to the bottom of the dish for about 15 min. Such neurones undergoing dissociation retained a short portion of their proximal dendrites.

Slice preparation

Wistar rats (10–30 days old) were decapitated under pentobarbital anaesthesia (50 mg kg^{-1}, I.P.). The lumbar enlargement of the spinal cord was quickly removed and transversely sliced at a thickness of 250 μm using a microslicer (VT1000S, Leica, Germany) in a cold low-

Na$^+$ medium (see below). The slices were kept in an incubation medium saturated with 95% O_2 and 5% CO_2 at 30–35 °C for at least 1 h. Thereafter the slices were transferred to a recording chamber, and lamina II of the dorsal horn was identified under an upright microscope (Axioscope, Zeiss, Germany). The bath solution was perfused at 8–10 ml min^{-1}.

All experiments conformed to the guiding principles for the care and use of animals approved by The Council of The Physiological Society of Japan, and all efforts were made to minimize the number of animals and their suffering.

Electrical measurements

Electrical measurements were performed on the dissociated neurones using the nystatin perforated patch recording mode and on the slice preparation using the conventional whole cell patch recording mode under voltage-clamp conditions. When the nystatin perforated patch recording mode was applied to the dissociated neurones, the technique allowed a long time for recordings, which was not possible using the conventional whole cell patch recording mode. In the slice preparation, however, the conventional whole cell patch technique was applied because this technique is easier and more convenient, and gave sufficient time to record cell response. All voltage-clamp recordings were made at a holding potential (V_H) of −60 mV (CEZ-2300, Nihon Kohden, Tokyo, Japan). Patch pipettes were made from borosilicate capillary glass (1.5 mm o.d., 0.9 mm i.d.; G-1.5, Narishige, Tokyo, Japan) in two stages on a vertical pipette puller (PB-7, Narishige, Japan). The resistance of the recording pipettes when filled with internal solution was 5–6 MΩ. Neurones were viewed under phase contrast on an inverted microscope (Diaphot, Nikon, Japan). Current and voltage were continuously monitored on an oscilloscope (VC-6023, Hitachi, Japan), a pen recorder (RECTI-HORIT-8K, Sanei, Tokyo, Japan) and recorded on a digital-audio tape recorder (RD-120TE, TEAC, Japan). Membrane currents were filtered at 1 kHz (E-3201A Decade Filter, NF Electronic Instruments, Tokyo, Japan), digitized at 4 kHz, and stored on an off-line computer equipped with pCLAMP 8.0 (Axon Instruments, Germany). All experiments were performed at room temperature (22–24 °C), except for the slice preparation (32–35 °C).

Electrical stimulations used to obtain evoked glycinergic IPSCs (eIPSCs) were performed by applying short (100 μs) voltage pulses at 0.1 Hz through a glass pipette (i.d., 10 μm). The pipette was placed in the lamina II region and filled with the incubation medium using the PULSE program on a computer. The signals were filtered at 3 kHz and digitized at 10 kHz.

Data analysis

Spontaneous miniature inhibitory postsynaptic currents (mIPSCs) were counted and analysed using the MiniAnalysis Program (Synaptosoft, Decatur, GA, USA). Spontaneous events were screened automatically using an amplitude threshold of 5 pA and then visually accepted or rejected based upon rise and decay times. The average value of mIPSC frequency during the control period (10–15 min) was calculated, and the frequency of all the events during agonist application (1–2 min) was normalized to this value. The effect of the drug was quantified as a percentage increase in mIPSC frequency compared to the control value, and the results were discarded when agonist actions showed apparent desensitization to repeated applications. The decay time was analysed for mIPSC events with a rise time of 1.0–1.5 ms, and this was well fitted to a single exponential function. The amplitudes and inter-event intervals of large numbers of spontaneous IPSCs obtained from a single neurone were examined by constructing cumulative probability distributions and compared using the Kolmogorov-Smirnov (K-S) test. The continuous curves for concentration–

Table 1. The properties of glycinergic mIPSCs in SG neurones

Developmental stages	Frequency (Hz)	Amplitude (pA)	Decay time (ms)
P10–12	0.4 ± 0.15 ($n = 37$)	69.3 ± 7.1 ($n = 37$)	12.3 ± 0.7 ($n = 10$)
P16–18	0.5 ± 0.12 ($n = 67$)	71.8 ± 6.9 ($n = 67$)	12.2 ± 0.9 ($n = 10$)
P28–30	0.5 ± 0.13 ($n = 84$)	70.7 ± 6.4 ($n = 84$)	10.1 ± 0.7 ($n = 10$)

Values are means $\pm$ S.E.M.

response relationships were constructed according to a modified Michaelis-Menten equation, using a least-squares fitting routine:

$$F = F_{max} C^n / (C^n + EC_{50}{}^n),$$

where F is the agonist-elicited facilitation ratio of mIPSC frequency and C is the corresponding agonist concentration. EC_{50} and n denote the half-effective concentration and Hill coefficient, respectively. Differences in amplitude and frequency distribution were tested by Student's paired two-tailed t test using their absolute values. Numerical values were provided as the mean $\pm$ standard error of the mean (S.E.M.). Values of $P < 0.05$ were considered significant.

Solutions

The incubation medium consisted of (mM): 124 NaCl, 5 KCl, 1.2 KH$_2$PO$_4$, 24 NaHCO$_3$, 2.4 CaCl$_2$, 1.3 MgSO$_4$ and 10 glucose bubbled with 95 % O$_2$ and 5 % CO$_2$. The pH was about 7.45. The standard external solution consisted of (mM): 150 NaCl, 5 KCl, 2 CaCl$_2$, 1 MgCl$_2$, 10 glucose and 10 Hepes. The low-Na$^+$ medium consisted of 230 sucrose, 2.5 KCl, 1.25 Na$_2$HPO$_4$, 10 MgSO$_4$, 0.5 CaCl$_2$, 26 NaHCO$_3$ and 30 glucose. Ca^{2+}-free external solution consisted of (mM): 150 NaCl, 5 KCl, 5 MgCl$_2$, 2 EGTA, 10 glucose and 10 Hepes. These external solutions were adjusted to pH 7.4 with Tris-base. In recording mIPSCs, external solutions routinely contained 3×10^{-7} M tetrodotoxin (TTX) to block voltage-dependent Na$^+$ channels and 3×10^{-6} M 6-cyano-7-nitroquinoxaline-2,3-dione (CNQX), 10^{-5} M DL-2-amino-5-phosphovaleric acid (AP5) and 3×10^{-6} M bicuculline to block glutamatergic and GABAergic currents, respectively. The ionic composition of the internal (patch pipette) solution for the nystatin-perforated patch recording was (mM): 40 caesium methanesulfonate, 5 MgCl$_2$, 100 CsCl and 10 Hepes with pH adjusted to 7.2 with Tris-base. Nystatin was dissolved in acidified methanol at 10 mg ml^{-1}. This stock solution was diluted with the internal solution just before use to a final concentration of 100–200 μg ml^{-1}. The ionic composition of the internal solution for whole cell patch recording was (mM): 92 caesium methanesulfonate, 43 CsCl, 5 TEA-Cl, 2 EGTA, 4 ATP-Mg and 10 Hepes with pH adjusted to 7.2 with Tris-base.

Drugs

The drugs used in the present study were AP5, bicuculline, CNQX, TTX, EGTA, nystatin, Na-ATP, pyridoxal-5-phosphate-6-azophenyl-2′,4′-disulfonic acid (PPADS), reactive blue-2 (RB-2), strychnine, thapsigargin, substance P (SP) and $\alpha\beta$-methylene-ATP ($\alpha\beta$-me-ATP) from Sigma (USA); 2-methylthio-ATP (2MeS-ATP), calcitonin gene-related peptide (CGRP) and *trans*-($\pm$)-1-amino-1,3-cyclopentane-dicarboxylic acid (t-ACPD) from RBI (USA); 2′,3′-*O*-(2,4,6-trinitrophenyl)-ATP (TNP-ATP) from Molecular Probes (USA). CNQX and bicuculline were dissolved in dimethyl sulfoxide at 10 mM as a stock solution. All solutions containing drugs were applied using the 'Y-tube' perfusion system for rapid solution exchange within 20 ms (Akaike & Harata, 1994). In all experiments, either ATP or related agonists were applied at intervals of more than 20 min to allow the full recovery of presynaptic effects (see also Results).

RESULTS

Glycinergic mIPSCs

To examine whether ATP receptor subtypes do change during postnatal development, we divided the specimens into three age groups: postnatal days 10–12 (P10–12), P16–18 and P28–30. The reasons for this division are as follows. First, many physiological systems develop quickly in the first 2 postnatal weeks. Second, previously our results suggested that only the P2X2 receptor subtype is involved in the modulation of spontaneous glycinergic transmission. Third, most of the binding or immunohistochemical studies showing that multiple P2X subunit RNAs are expressed in the dorsal horn have been conducted in adult rats (Collo *et al.* 1996; Vulchanova *et al.* 1996, 1997).

In the presence of 3×10^{-7} M TTX, 3×10^{-6} M CNQX, 10^{-5} M AP5 and 3×10^{-6} M bicuculline, the spontaneous miniature postsynaptic currents recorded from P28–30 neurones were completely blocked by 10^{-6} M strychinine (Fig. 1*A*). Figure 1*B* shows typical mIPSCs at various holding potentials and their current–voltage (I–V) relationship. The reversal potential of these mIPSCs, as estimated from the I–V relationship, was about -10.0 ± 0.32 mV ($n = 4$), which was almost identical to the theoretical Cl$^-$ equilibrium potential (E_{Cl}) of -10.4 mV calculated by the Nernst equation using extra- and intracellular Cl$^-$ concentrations (161 mM [Cl$^-$]$_o$ and 110 mM [Cl$^-$]$_i$, respectively). The results indicate that the spontaneous postsynaptic currents are glycinergic miniature inhibitory postsynaptic currents (mIPSCs).

Table 1 shows the properties of glycinergic mIPSCs obtained from each developmental stage. Both the mIPSC frequencies and amplitudes showed no significant difference among these three groups ($P > 0.05$, Student's unpaired t test). In addition, there is no significant correlation between the decay time constants and the postnatal stage when fitted by linear regression ($r^2 = 0.139$, $P > 0.05$, Student's unpaired t test). In summary, the sensitivity of glycine receptors in postsynaptic neurones and the glycine release from the presynaptic nerve terminals hardly changed during all the stages tested.

Multiple effects of ATP or $\alpha\beta$-me-ATP on SG neurones during maturation

Previous results indicated that ATP activates presynaptic P2X receptors on the glycinergic nerve terminals and/or postsynaptic P2X receptors on the SG neurone soma (Rhee *et al.* 2000). In order to understand more fully the changes in ATP response during neuronal maturation, we have investigated the effects of ATP or $\alpha\beta$-me-ATP in three developmental stages. In the majority of neurones

tested, regardless of stage of maturation, ATP (10^{-4} M) markedly increased the mIPSC frequency without eliciting any postsynaptic inward currents (Fig. 2*Aa*). In a small number of neurones tested, ATP elicited postsynaptic inward currents in addition to an increase of mIPSC frequency (Fig. 2*Ab*). In a subset of neurones, ATP elicited only postsynaptic inward currents (Fig. 2*Ac*). In the remaining neurones, ATP had no effect (Fig. 2*Ad*). Table 2 shows the results obtained from each
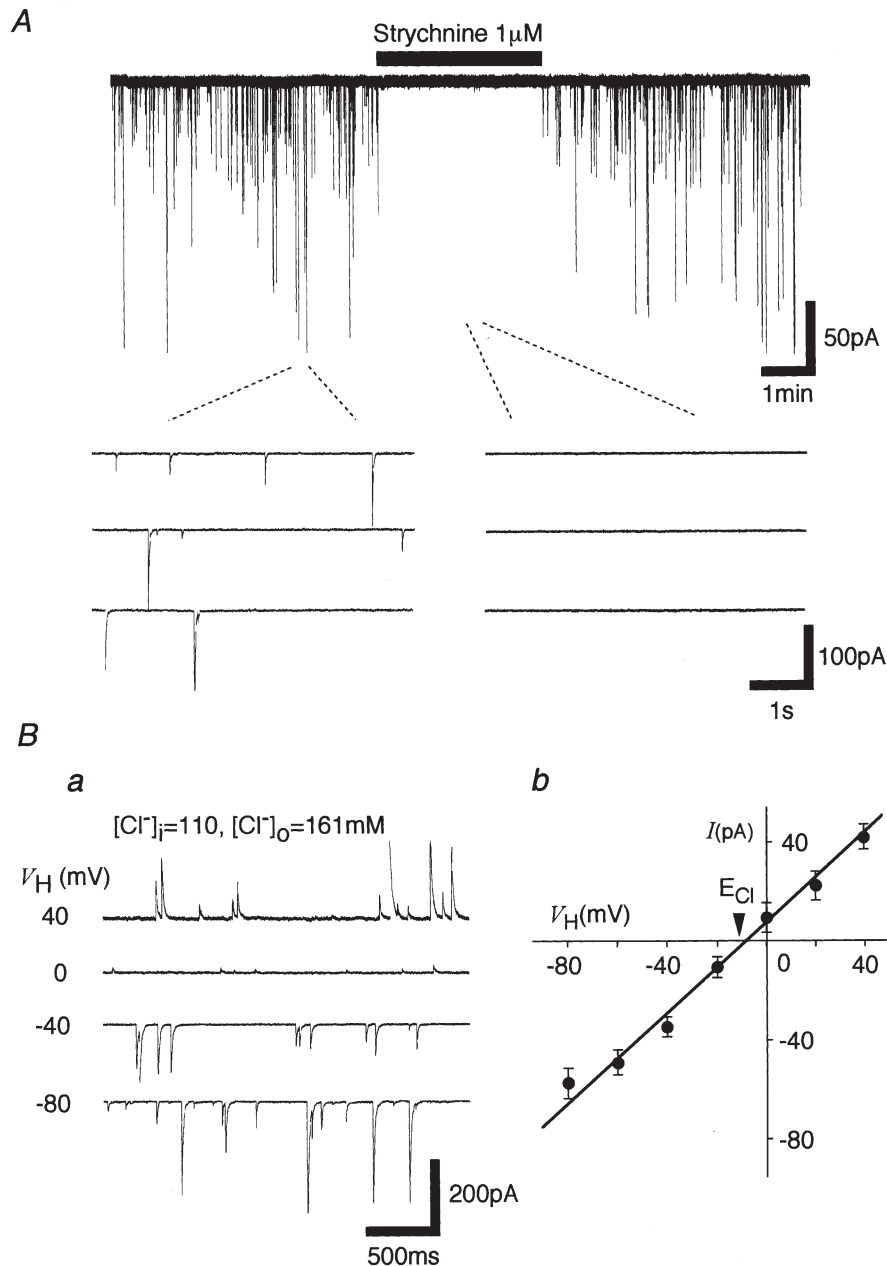

Figure 1. Glycinergic mIPSCs

A, typical spontaneous miniature postsynaptic currents (mIPSCs) observed before, during and after the application of 10^{-6} M strychnine in the presence of 3×10^{-7} M TTX, 3×10^{-6} M CNQX, 10^{-5} M AP5 and 3×10^{-6} M bicuculline. Insets indicate the current recordings with an expanded time scale. *Ba*, typical traces recorded from a neurone at various holding potentials. *Bb*, the *I–V* relationship in which each point is the mean of 4 neurones.
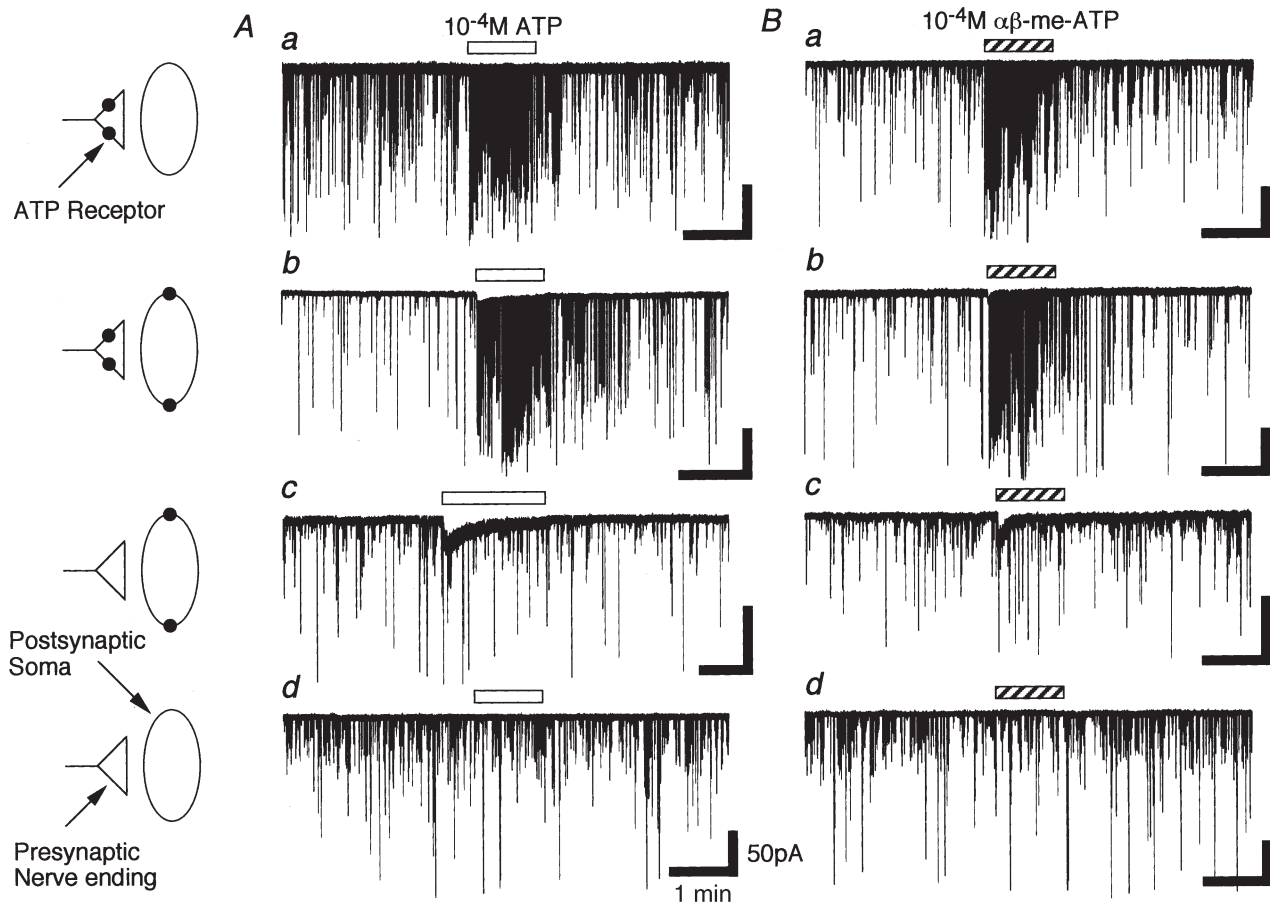
Table 2. The incidence of ATP or $\alpha\beta$-me-ATP-elicited responses during postnatal development

	ATP sensitive			$\alpha\beta$-me-ATP sensitive		
	P10–12	P16–18	P28–30	P10–12	P16–18	P28–30
Presynaptic	58 (65.2)	78 (64.5)	61 (61.7)	0 (0)	12 (19.3)	92 (46.9)
Postsynaptic	6 (6.7)	8 (6.6)	14 (14.1)	0 (0)	7 (11.3)	24 (12.2)
Pre- and postsynaptic	5 (5.6)	10 (8.3)	14 (14.1)	0 (0)	6 (9.7)	28 (14.3)
No effect	20 (22.5)	25 (20.6)	10 (10.1)	42 (100)	37 (59.7)	52 (26.5)
Total number of responses	89 (100)	121 (100)	99 (100)	42 (100)	62 (100)	196 (100)

Values in parentheses are a percentage of the total number of responses.

developmental stage. The number of neurones which exhibit postsynaptic responses increased while ATP-insensitive neurones decreased. These results indicate that ATP-sensitive neurones consistently increase with maturation. $\alpha\beta$-me-ATP (10^{-4} M) did not elicit either presynaptic or postsynaptic responses in P10–12 neurones (Table 2, see also Rhee *et al.* 2000). In later developmental stages, however, $\alpha\beta$-me-ATP mimicked ATP-elicited presynaptic or postsynaptic effects, and $\alpha\beta$-me-ATP-sensitive neurones also increased with maturation (Fig. 2*B* and Table 2). In the P28–30 group, all $\alpha\beta$-me-ATP-sensitive neurones tested (38/38, 100 %) were sensitive to ATP, while some of the ATP-sensitive neurones tested (11/76, 14 %) were insensitive to $\alpha\beta$-me-

Figure 2. ATP- and $\alpha\beta$-me-ATP-elicited multiple responses

A, the incidence of four kinds of ATP-elicited responses including only presynaptic action (*a*), presynaptic and postsynaptic actions (*b*), only postsynaptic action (*c*) and no action (*d*) in P28–30 neurones. *B*, the incidence of four kinds of $\alpha\beta$-me-ATP-elicited responses including only presynaptic action (*a*), presynaptic and postsynaptic actions (*b*), only postsynaptic action (*c*) and no action (*d*). Note that $\alpha\beta$-me-ATP-elicited postsynaptic currents were more quickly desensitized than ATP-elicited postsynaptic currents.

ATP. This suggests that a subset of P28–30 neurones expresses $\alpha\beta$-me-ATP-insensitive ATP receptors. It should be noted that $\alpha\beta$-me-ATP elicited quickly desensitizing postsynaptic currents, whereas ATP elicited biphasic currents with a non-desensitizing plateau phase during the application (Fig. 2*Bb* and *c*).

Presynaptic effects of ATP and related agonists on SG neurones during maturation

To identify what kinds of ATP receptor subtypes are responsible for mIPSC frequency facilitation during maturation, the effects of alternative agonists were examined at each postnatal stage (Fig. 3*A*). ATP (10^{-4} M) increased the mIPSC frequency to $621.4 \pm 115.3\%$ in P10–12, $557.3 \pm 86.5\%$ in P16–18 and $594.1 \pm 141.3\%$ in P28–30 neurones. 2MeS-ATP (10^{-4} M) mimicked the ATP action and increased mIPSC frequency to $864.1 \pm 170.6\%$, $765.4 \pm 129.1\%$ and $851.6 \pm 100.3\%$ in P10–12, P16–18 and P28–30 neurones, respectively. Another P2X receptor agonist, $\alpha\beta$-me-ATP (10^{-4} M), had no effect on the mIPSC frequency and amplitude in P10–12 (see also Rhee *et al.* 2000). However, the facilitatory effect of $\alpha\beta$-me-ATP on mIPSC frequency was noted from P16–18 and increased with maturation. $\alpha\beta$-me-ATP increased mIPSC frequency to $340.5 \pm 87.6\%$ and $649.3 \pm 83.6\%$ in P16–18 and P28–30 neurones, respectively (Fig. 3*Ba*). On the other hand, the

mean amplitude of mIPSCs elicited by each agonist did not change with maturation (Fig. 3*Bb*).

To quantify ATP- and $\alpha\beta$-me-ATP-elicited presynaptic responses, we examined the effects of the repeated applications of agonists on mIPSC frequency. The results might be important particularly for determining concentration–response relationships or analysing the pharmacological properties of ATP receptor subtypes. Figure 4 shows how time intervals influenced agonist-elicited presynaptic responses during the repeated applications in P28–30 neurones. ATP- and $\alpha\beta$-me-ATP-elicited presynaptic responses were fully recovered at a interval of 20 min (Fig. 4*Aa* and *b*). In addition, $\alpha\beta$-me-ATP-elicited presynaptic responses were reproducible during the repeated applications, although they slightly decreased in the fourth application (Fig. 4*Ba* and *b*). In all experiments, therefore, either ATP or related agonists were applied at intervals of more than 20 min to allow the full recovery of their presynaptic responses.

Figure 5 shows how ATP and related agonists increase mIPSC frequency in a concentration-dependent manner at three developmental stages. The EC_{50} values of ATP were 4.9×10^{-6} M, 2.1×10^{-6} M and 1.7×10^{-6} M and those of 2MeS-ATP were 9.3×10^{-6} M, 1.7×10^{-5} M and 5.6×10^{-6} M in P10–12, P16–18 and P28–30 neurones, respectively. The potencies of ATP or 2MeS-ATP were
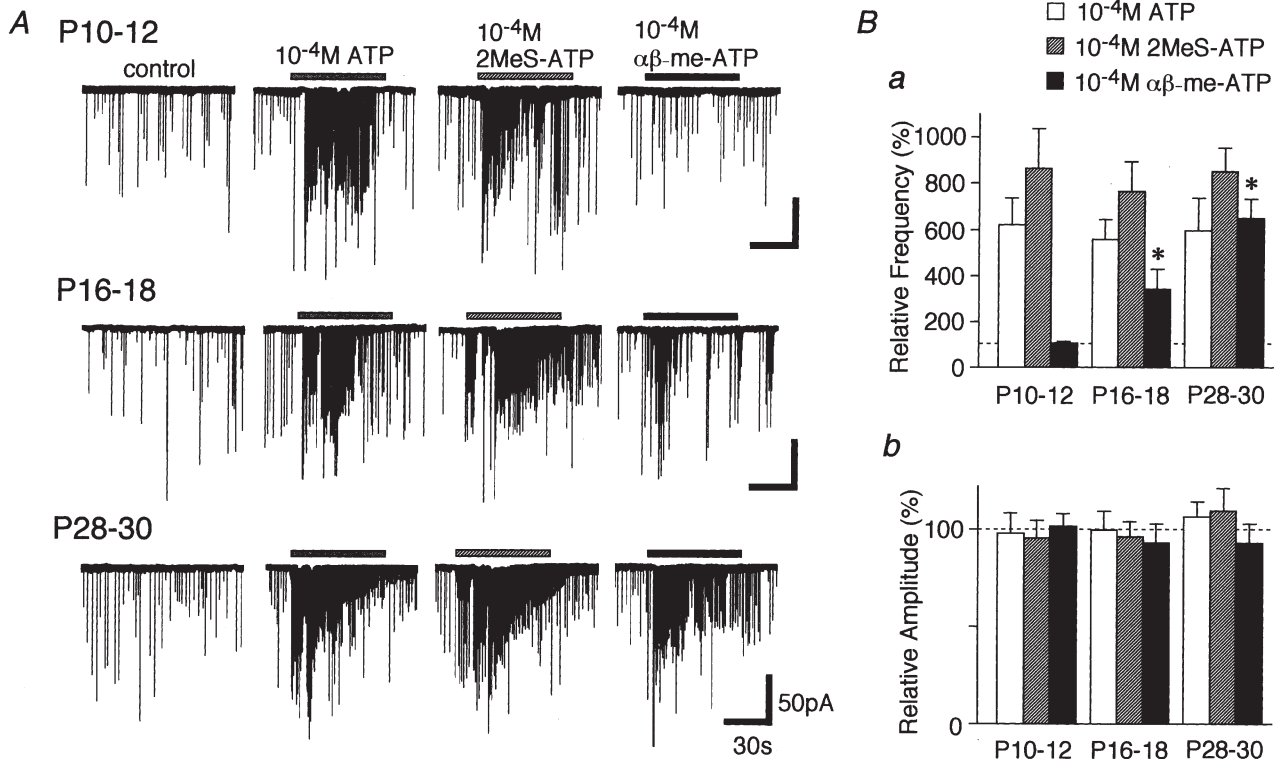

Figure 3. Developmental changes of agonist-elicited presynaptic responses

A, typical traces of mIPSCs induced by application of 10^{-4} M ATP, 2MeS-ATP and $\alpha\beta$-me-ATP. All recordings were obtained from a single neurone at different developmental stages. *B*, each column is the mean of 5–12 neurones and normalized to the respective control. *P < 0.05.
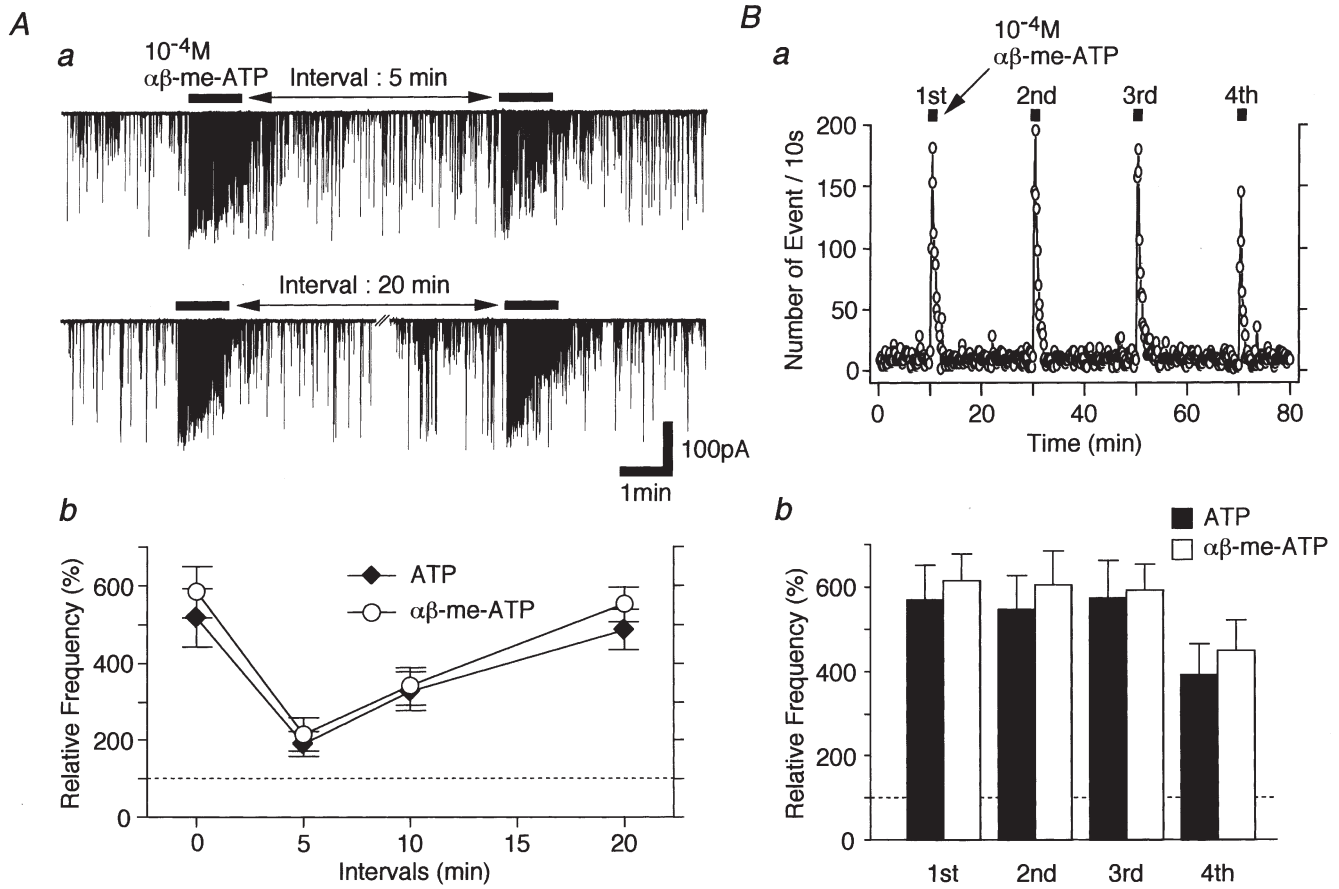
Figure 4. Time-dependent recovery of ATP- and $\alpha\beta$-me-ATP-elicited presynaptic responses

Aa, typical traces of mIPSCs induced by repeated applications of 10^{-4} M ATP at different time intervals. *Ab*, summary of time-dependent recovery of ATP- and $\alpha\beta$-me-ATP-elicited presynaptic responses. Note that ATP and $\alpha\beta$-me-ATP actions on mIPSC frequency were fully recovered after an interval of 20 min. *B*, the reproducibility of ATP- or $\alpha\beta$-me-ATP-elicited presynaptic responses. *Ba*, successive applications of 10^{-4} M $\alpha\beta$-me-ATP at 19 min intervals increased mIPSC frequency in a reproducible manner. The number of events every 10 s is plotted. *Bb*, each column is the mean of 4 neurones and normalized to the respective control.
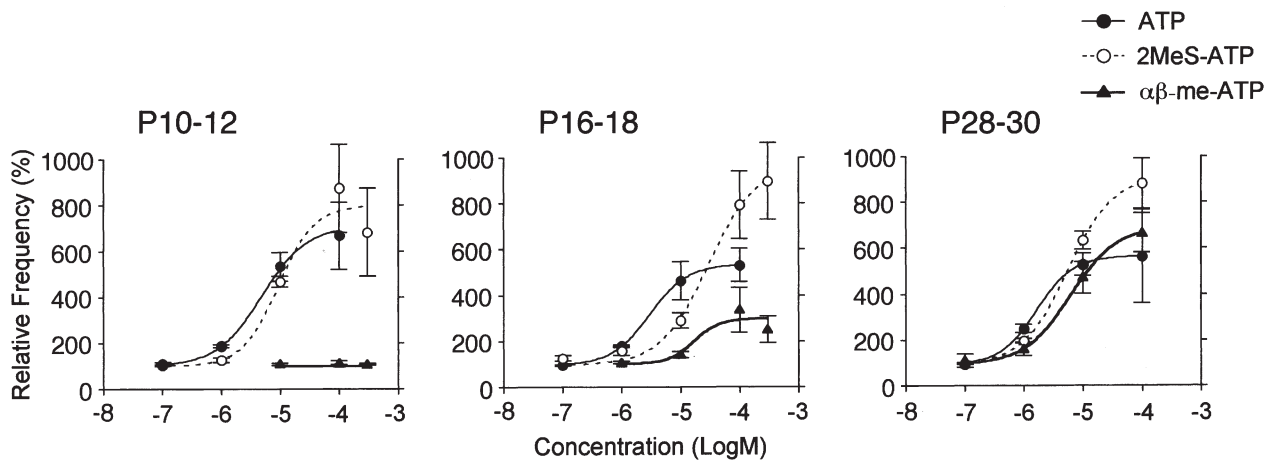

Figure 5. Concentration–response relationships for ATP and its agonists

Concentration–response relationships for ATP, 2MeS-ATP and $\alpha\beta$-me-ATP in P10–12, P16–18 and P28–30 neurones, respectively. All points ($n = 5$–12 neurones) are normalized to the respective control. The continuous lines represent the fit of the Hill function (see Methods).

the same throughout the three different stages. On the other hand, the facilitatory effect of $\alpha\beta$-me-ATP on mIPSC frequency was noted at P16–18. The EC_{50} values of $\alpha\beta$-me-ATP were 1.6×10^{-5} M in P16–18 and 6.2×10^{-6} M in P28–30 neurones (Fig. 5). The data suggest that $\alpha\beta$-me-ATP-sensitive ATP receptors appear with maturation. Accordingly, all of the following pharmacological experiments were performed with P28–30 neurones to determine the properties of $\alpha\beta$-me-ATP-sensitive ATP receptors.

Ionotropic action of $\alpha\beta$-me-ATP-elicited mIPSC frequency facilitation

We examined whether voltage-dependent Ca^{2+} channels (VDCCs) in the glycinergic nerve terminals participate in the facilitatory effect of $\alpha\beta$-me-ATP on mIPSC frequency in later developmental stages (Fig. 6). In the presence of 10^{-4} M Cd^{2+}, a concentration which completely blocks VDCCs, glycinergic mIPSC frequency was significantly reduced by $54.7 \pm 10.7\%$ of the control ($P < 0.01$, $n = 5$). This suggests that the VDCCs contribute to spontaneous glycine release from these presynaptic nerve terminals. In the presence of Cd^{2+}, either 10^{-4} M ATP or 10^{-4} M $\alpha\beta$-me-ATP could still facilitate the mIPSC frequency to 551.6 ± 102.0 and $590.1 \pm 130.5\%$ of the control Cd^{2+} condition ($P < 0.05$, $n = 5$), respectively (Fig. 6Aa and b). The results suggest that the ATP- and $\alpha\beta$-me-ATP-sensitive ATP receptors may be permeable to Ca^{2+} and that Ca^{2+} influxes through ATP receptors may directly contribute to the facilitation of glycine release. Thus, the effects of ATP and $\alpha\beta$-me-ATP were examined in P28–30 neurones immersed in the Ca^{2+}-free external solution (Fig. 6B and C). Ca^{2+}-free external solution itself also reduced the mIPSC frequency
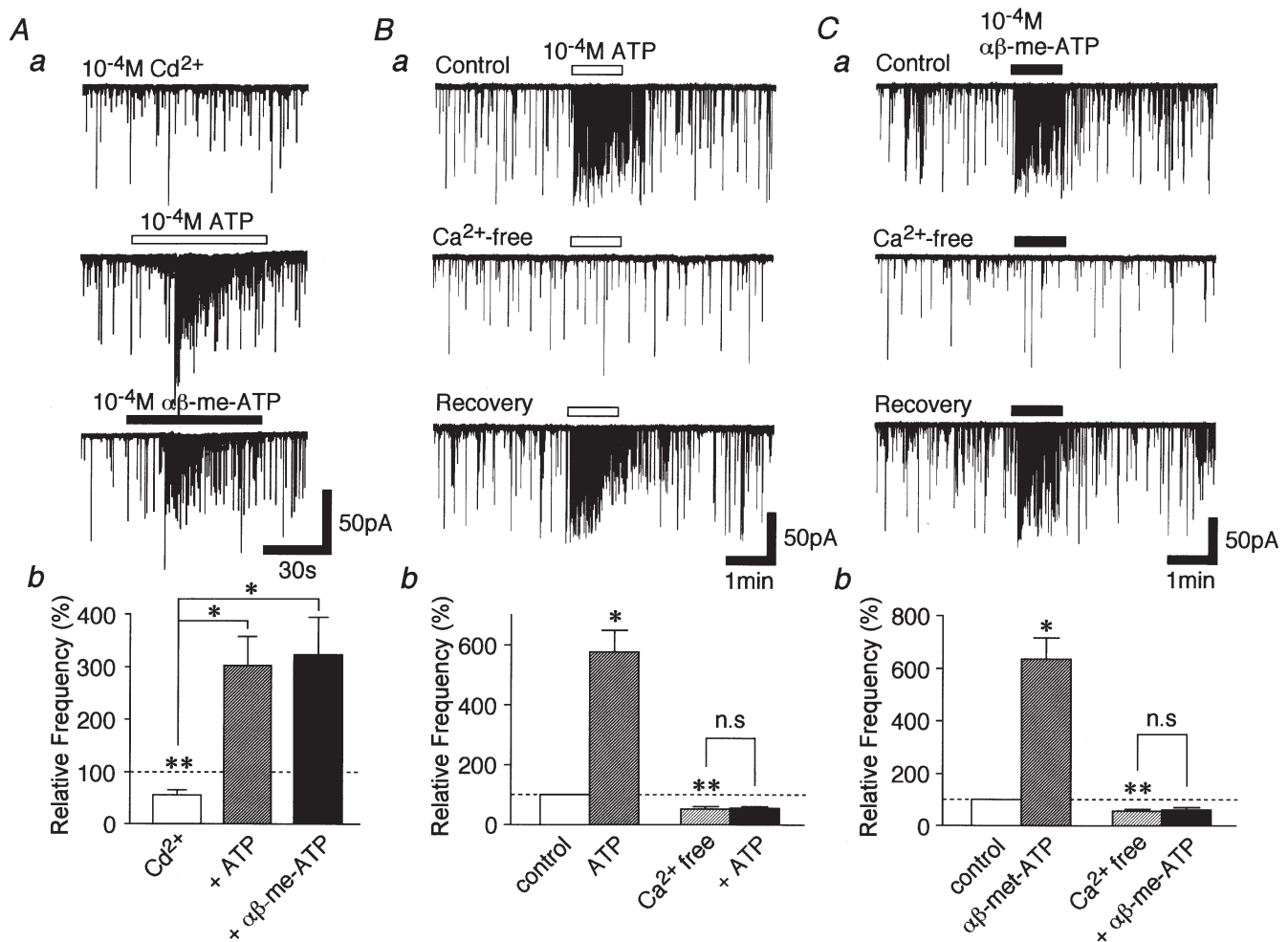

Figure 6. Effects of Cd^{2+} and Ca^{2+}-free external solution on ATP- and $\alpha\beta$-me-ATP-elicited glycinergic mIPSC frequency facilitation

Aa, typical traces of mIPSCs observed from a P28–30 neurone after the application of 10^{-4} M ATP or $\alpha\beta$-me-ATP in the presence of 10^{-4} M Cd^{2+}. *Ab*, each column is the mean of 5 neurones. All columns are normalized to the control. *$P < 0.05$, **$P < 0.01$. *B* and *C*, typical traces of mIPSCs observed from a P28–30 neurone in the Ca^{2+}-free external solution after the application of 10^{-4} M ATP (*Ba*) and $\alpha\beta$-me-ATP (*Ca*). Pooled data for ATP (*Bb*, $n = 5$) and $\alpha\beta$-me-ATP (*Cb*, $n = 4$) are presented. Each column is normalized to the control. *$P < 0.05$, **$P < 0.01$.

to $55.6 \pm 7.1\%$ of the control ($P < 0.01$, $n = 5$, Fig. 6*Bb* and *Cb*). The decrease of mIPSC frequency was nearly the same as that observed in the Cd^{2+} solution. In the Ca^{2+}-free external solution, however, the facilitatory effects of either 10^{-4} M ATP or $\alpha\beta$-me-ATP on the mIPSC frequency were completely abolished (Fig. 6*B* and *C*, $P > 0.05$, $n = 5$).

To confirm that $\alpha\beta$-me-ATP-elicited mIPSC frequency facilitation is mediated by ionotropic P2X but not metabotropic P2Y receptors, we tested the effect of thapsigargin, which blocks the sarcoplasmic/endoplasmic reticulum Ca^{2+}-ATPase and inhibits the Ca^{2+} refilling of intracellular stores. Thapsigargin (10^{-6} M) itself increased mIPSC frequency to $179.6 \pm 23.3\%$ of the control ($P < 0.05$, $n = 5$) without affecting mIPSC mean amplitude (Fig. 7*C*). This effect might be due to the thapsigargin-induced Ca^{2+} release from intracellular Ca^{2+} stores. However, $\alpha\beta$-me-ATP (10^{-4} M) still facilitated mIPSC frequency to $571.0 \pm 84.2\%$ of the thapsigargin condition (Fig. 7*B* and *Cb*).
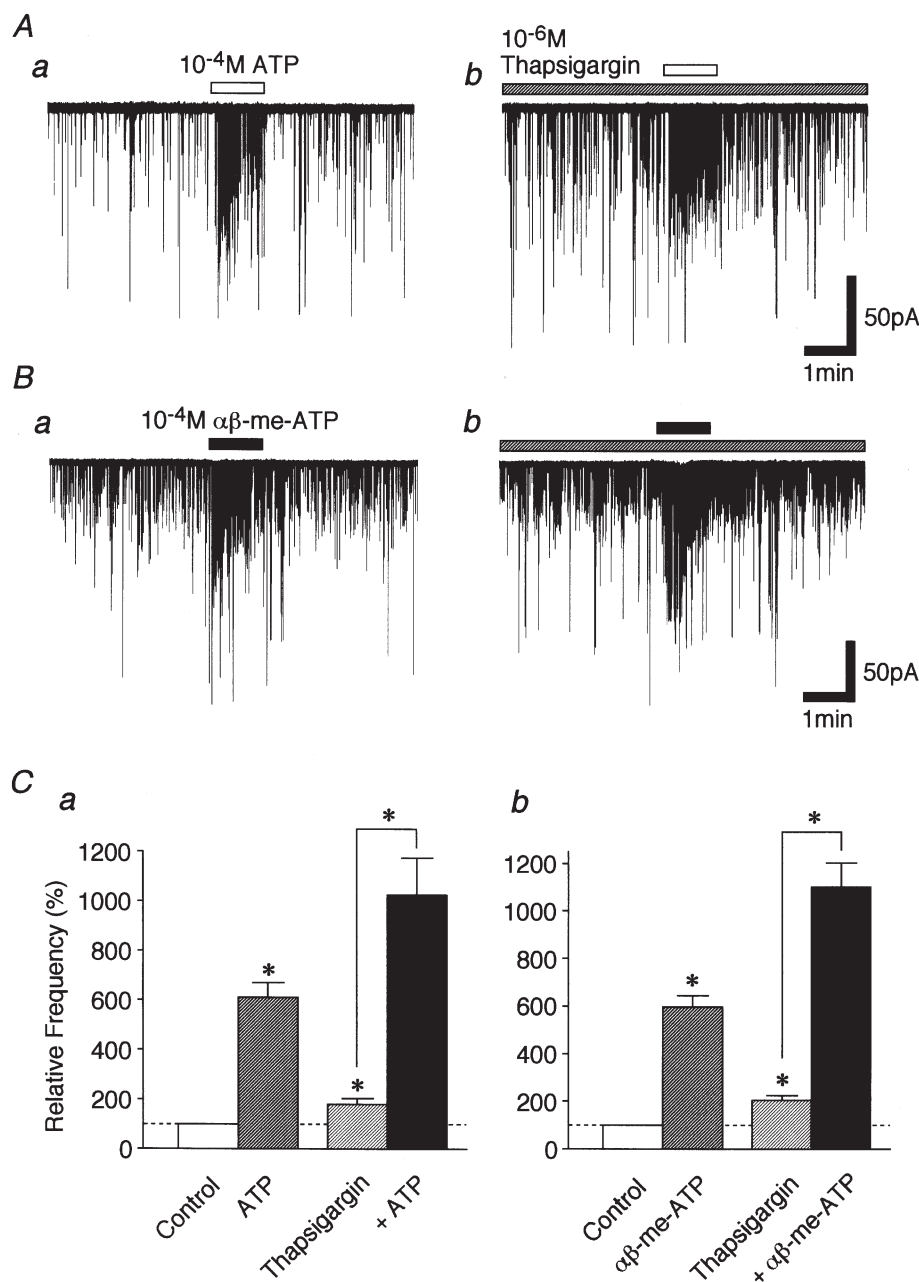

Figure 7. Effect of thapsigargin on ATP- and $\alpha\beta$-me-ATP-elicited glycinergic mIPSC frequency facilitation

A and *B*, typical traces of mIPSCs recorded during the application of 10^{-4} M ATP (*A*) and $\alpha\beta$-me-ATP (*B*) in the absence (*a*) and presence (*b*) of 10^{-6} M thapsigargin. *C*, each column is the mean of 5 neurones. All columns are normalized to the control. *$P < 0.05$.

Pharmacological properties of ATP- and $\alpha\beta$-me-ATP-elicited postsynaptic and presynaptic responses

Firstly, we tested the effect of P2X receptor antagonists, such as TNP-ATP and PPADS, on ATP- and $\alpha\beta$-me-ATP-elicited postsynaptic currents in P28–30 neurones (Fig. 8). PPADS at low micromolar concentrations is insensitive to both P2X4 and P2X6 receptors, and TNP-ATP at nanomolar concentrations is a potent antagonist

for P2X1, P2X3, heteromeric P2X2/3 and P2X1/5 receptors (Virginio *et al.* 1998). ATP-elicited postsynaptic currents (Fig. 8Aa) were partially blocked by adding 10^{-7} M TNP-ATP ($n = 4$, Fig. 8Ab) and completely occluded by the cumulative application of 10^{-5} M PPADS in addition to TNP-ATP ($n = 4$, Fig. 8Ac). However, ATP-elicited postsynaptic currents were completely blocked by adding 10^{-5} M PPADS alone ($n = 3$, not
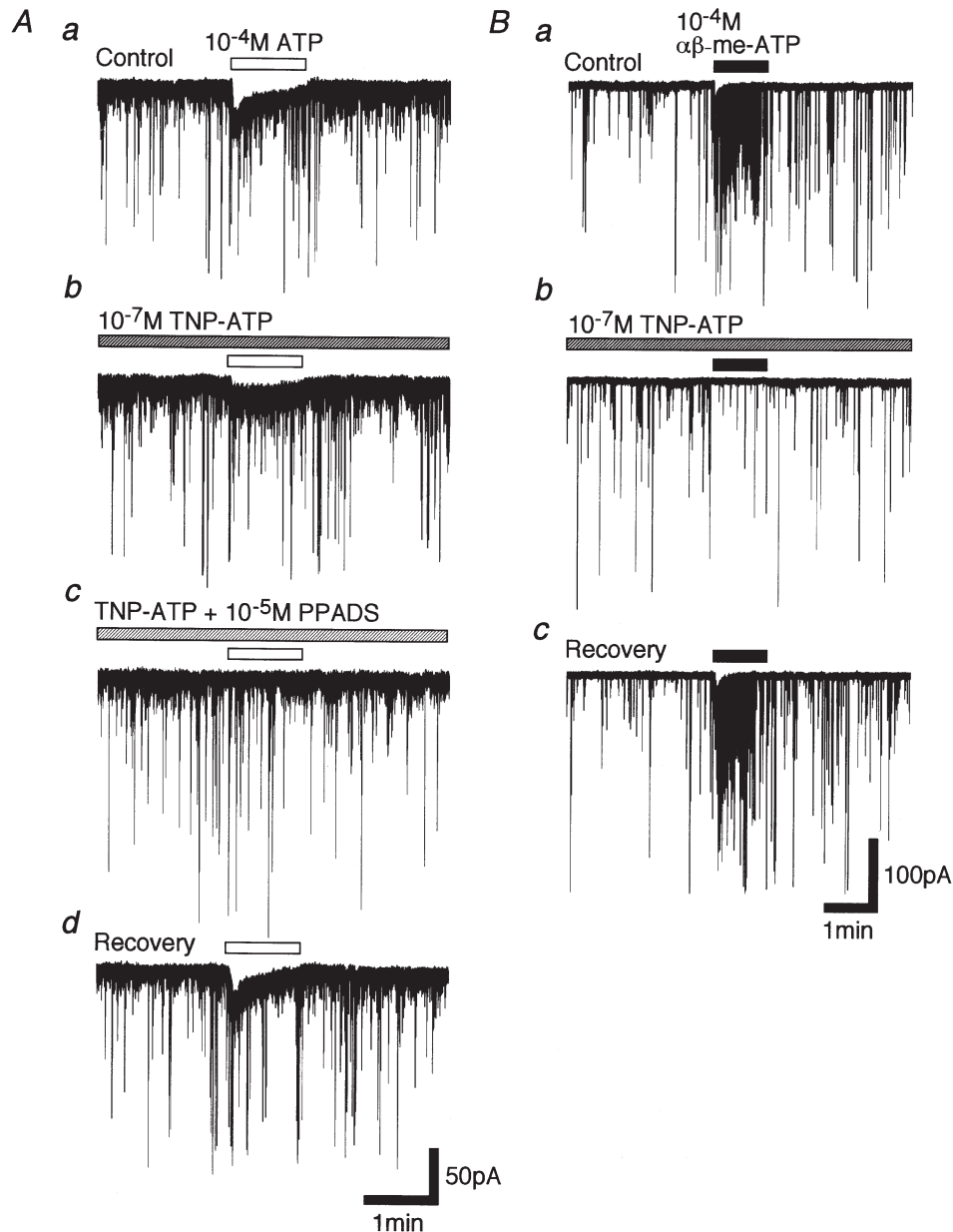

Figure 8. Effects of P2X receptor antagonists on ATP- and $\alpha\beta$-me-ATP-elicited postsynaptic currents

A, typical traces of 10^{-4} M ATP-elicited postsynaptic currents in the absence of any antagonists (*a*), and in the presence of 10^{-7} M TNP-ATP (*b*) and both 10^{-7} M TNP-ATP and 10^{-5} M PPADS (*c*). In *d*, ATP-elicited postsynaptic current was clearly recovered after washing out antagonists. *B*, typical traces of 10^{-4} M $\alpha\beta$-me-ATP-elicited postsynaptic currents in the absence of any antagonists (*a*), and in the presence of 10^{-7} M TNP-ATP (*b*). In *c*, $\alpha\beta$-me-ATP-elicited postsynaptic current was clearly recovered after washing out TNP-ATP.

shown). On the other hand, $\alpha\beta$-me-ATP-elicited postsynaptic currents (Fig. 8Ba) were completely blocked by adding either TNP-ATP ($n = 4$, Fig. 8Bb) or PPADS ($n = 3$, not shown). All antagonisms were reversible (Fig. 8Ad and Bc).

Previous results indicated that the facilitatory effect of ATP on mIPSCs in P10–13 neurones is completely blocked by PPADS (Rhee *et al.* 2000). In the present study performed on P28–30 neurones, 10^{-5} M PPADS blocked the ATP-elicited increase in glycinergic mIPSC frequency to $123.6 \pm 31.9\%$ of the PPADS condition ($P > 0.05$, $n = 6$), but 10^{-7} M TNP-ATP partially blocked this increase to $303.6 \pm 40.8\%$ of the TNP-ATP condition ($P < 0.05$, $n = 6$) (Fig. 9A). Interestingly, PPADS and TNP-ATP reversibly blocked the $\alpha\beta$-me-ATP-elicited increase of glycinergic mIPSC frequency to 129.8 ± 28.4 and $130.7 \pm 37.3\%$ of the respective drug conditions

($P > 0.05$, $n = 6$, Fig. 9B). Reactive blue 2 (RB-2, 10^{-5} M) partially blocked ATP- and $\alpha\beta$-me-ATP-elicited presynaptic responses to $235.6 \pm 46.8\%$ and $296.3 \pm 62.5\%$ of the RB-2 condition, respectively ($P < 0.05$, $n = 4$, respectively, Fig. 9Ac and Bc). On the other hand, glycinergic mIPSC frequency was not changed by PPADS, TNP-ATP or RB-2 (data not shown).

To elucidate the physiological significance of the present findings, the effect of $\alpha\beta$-me-ATP on evoked glycinergic IPSCs (eIPSCs) was tested on the slice preparation using the whole cell patch recording technique at V_H of -60 mV (Fig. 10). Since lamina II interneurones are known to make local inhibitory circuits within the dorsal horn area (Todd, 1988; Li *et al.* 1999), a glass pipette for electrical stimulation was placed near to the lamina II area. In P28–30 neurones, $\alpha\beta$-me-ATP (10^{-5} M) significantly reduced eIPSC amplitude to $68.8 \pm 10.6\%$ of control
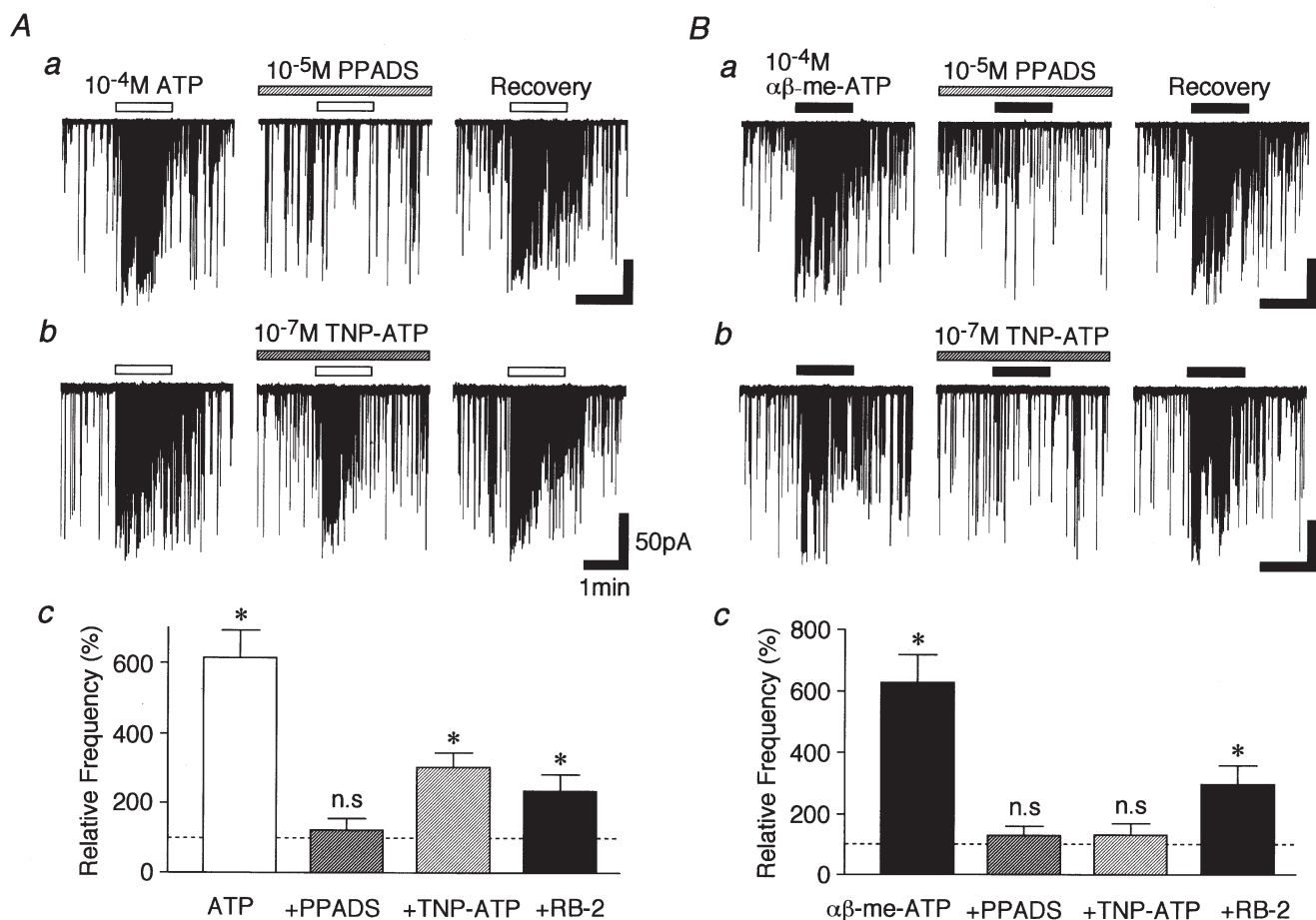

Figure 9. Effects of P2X receptor antagonists on ATP- and $\alpha\beta$-me-ATP-elicited presynaptic responses

A, typical traces of mIPSCs observed after the application of 10^{-4} M ATP in the presence of either 10^{-5} M PPADS (a) or 10^{-7} M TNP-ATP (b). Ac, each column is the mean of 5 neurones. All columns are normalized to their respective control. Note that ATP-induced facilitation of mIPSCs was completely blocked by PPADS, but partially blocked by TNP-ATP. *$P < 0.05$. B, typical traces of mIPSCs observed after the application of 10^{-4} M $\alpha\beta$-me-ATP in the presence of PPADS (a) or TNP-ATP (b). Bc, each column is the mean of 4 neurones and normalized to its respective control. Note that $\alpha\beta$-me-ATP-induced facilitation of mIPSCs was completely blocked by either TNP-ATP or PPADS. *$P < 0.05$.

($P < 0.05$, $n = 6$, Fig. 10*A* and *B*), although it facilitated spontaneous glycine release (Fig. 10*Ca* and *b*). This inhibitory action was probably not due to the postsynaptic mechanism, since the distribution of spontaneous IPSC amplitude did not change during the application of $\alpha\beta$-me-ATP (Fig. 10*Cb*). On the contrary, $\alpha\beta$-me-ATP had no effect on glycinergic eIPSCs in P10–12 neurones ($n = 4$, Fig. 10*A* and *B*).

DISCUSSION

Developmental changes of ATP- and $\alpha\beta$-me-ATP-elicited responses

In the present study, we have investigated whether other P2X receptor subtypes can modulate spontaneous glycinergic transmission during postnatal development. We have previously revealed that $\alpha\beta$-me-ATP did not elicit any presynaptic or postsynaptic effects in P10–13 dorsal horn neurones (Rhee *et al.* 2000). These results are consistent with our present results performed on P10–12

neurones. With maturation, however, while the number of ATP-sensitive neurones did not change, $\alpha\beta$-me-ATP could modulate the glycine release from P16–18 neurones and had nearly the same ability to facilitate glycinergic mIPSCs for ATP and $\alpha\beta$-me-ATP in P28–30 neurones. The results indicate that the glycinergic presynaptic terminals might express $\alpha\beta$-me-ATP-sensitive P2X receptors in the later developmental stages. Since $\alpha\beta$-me-ATP-elicited presynaptic responses were greater in P28–30 neurones than in P16–18 neurones, there might be a progressive expression of $\alpha\beta$-me-ATP-sensitive components on glycinergic nerve terminals.

In a small number of P28–30 neurones tested, $\alpha\beta$-me-ATP elicited quickly desensitizing postsynaptic inward currents, whose pharmacological properties were nearly consistent with those of presynaptic response (Figs 8 and 9). These results strongly suggest that a subset of dorsal horn neurones express $\alpha\beta$-me-ATP-sensitive P2X receptors. Since previous morphological studies suggest
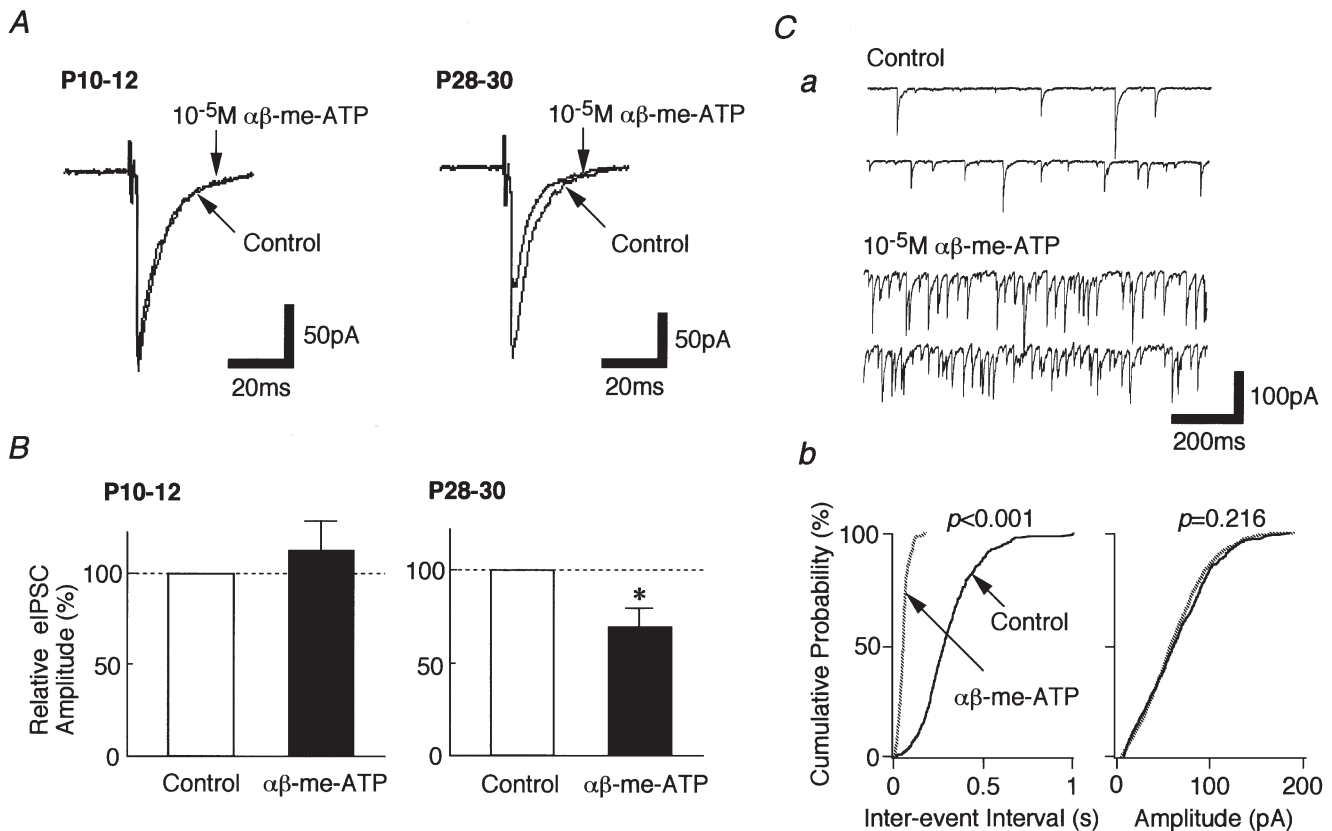

Figure 10. Effect of $\alpha\beta$-me-ATP on glycinergic eIPSCs

All recordings were performed in the slice preparation using the whole cell patch clamp technique. The incubation medium contained 10^{-5} M CNQX, 10^{-5} M AP5 and 10^{-5} M bicuculline, but not TTX. *A*, typical recordings of eIPSCs obtained from P10–12 neurones (left) and P28–30 neurones (right). *B*, each column is the mean of 4 (P10–12) and 6 (P28–30) neurones and was normalized to its respective control. **P < 0.05*. *Ca*, typical traces of mIPSCs observed before and during the application of 10^{-5} M $\alpha\beta$-me-ATP. *Cb*, cumulative probability plots for inter-event interval (left) and amplitude (right) of spontaneous IPSCs obtained from the same neurone. *P* values indicate the results of K-S test for frequency and amplitude (908 events for control and 1518 events for $\alpha\beta$-me-ATP).

that a subset of lamina II inhibitory interneurones make local inhibitory circuits within the dorsal horn (Todd, 1988; Li *et al.* 1999), most, but not all, $\alpha\beta$-me-ATP-sensitive glycinergic nerve terminals might originate from dorsal horn interneurones. In addition, the present results (Fig. 10) partly support the previous findings. However, it should be noted that neurones sensitive to $\alpha\beta$-me-ATP were also sensitive to ATP, but some of the ATP-sensitive neurones tested (11/76, 14%) were insensitive to $\alpha\beta$-me-ATP. Since ATP is a common agonist for all P2X receptors, but $\alpha\beta$-me-ATP is for only P2X1, P2X3, P2X1/5, P2X2/3 and P2X4/6 receptors (for review see Khakh *et al.* 2001), some of the SG neurones are likely to express $\alpha\beta$-me-ATP-sensitive P2X receptors, while others express $\alpha\beta$-me-ATP-insensitive P2X receptors in later developmental stages.

$\alpha\beta$-me-ATP activates ionotropic P2X receptors

The $\alpha\beta$-me-ATP-sensitive ATP receptor responsible for facilitating the mIPSCs required extracellular Ca^{2+} but did not require the voltage-gated Ca^{2+} channels in P28–30 neurons (Fig. 6), suggesting that the enhancement of mIPSC frequency results from Ca^{2+} influxes through $\alpha\beta$-me-ATP-sensitive receptors. In dorsal horn astrocytes, thapsigargin blocks ATP-elicited increase of intracellular Ca^{2+} concentration mediated by P2Y receptor activation (Salter & Hicks, 1995). The present results showing that thapsigargin had no effect on $\alpha\beta$-me-ATP-elicited presynaptic responses support the absence of a relationship with P2Y receptor activation. Accordingly, $\alpha\beta$-me-ATP may activate ionotropic P2X receptors on the glycinergic presynaptic nerve terminals, thus facilitating spontaneous glycine release at these synapses.

Pharmacological properties of $\alpha\beta$-me-ATP-sensitive P2X receptors

Although seven P2X receptor subunits have been cloned, it is hard to distinguish pharmacologically each subtype because of limited subunit-specific agonists and antagonists (for review see North & Barnard, 1997; Khakh *et al.* 2001). In the present study, the $\alpha\beta$-me-ATP-elicited increase of mIPSC frequency was completely blocked by adding either PPADS or nanomolar TNP-ATP (Fig. 8). Such pharmacological properties are almost consistent with the those of P2X1, P2X3, P2X2/3 and P2X1/5 receptors (Virginio *et al.* 1998; Torres *et al.* 1998). The immunohistochemical study of adult rats using subtype-specific antisera has suggested the existence of P2X1 and P2X3 immunoreactivity localized in the sensory ganglia and the superficial laminae of the dorsal horn. However, it is likely that P2X1 and P2X3 receptor subunits are in the central terminals of sensory afferent processes (Vulchanova *et al.* 1996, 1997, 1998). In addition, *in situ* hybridization study has revealed that both P2X1 and P2X3 subunit RNAs are not found in the spinal cord dorsal horn region of adult rat (Collo *et al.* 1996). Therefore, it might be reasonable to assume that

P2X1, P2X3, P2X2/3 or P2X1/5 receptors are not $\alpha\beta$-me-ATP-sensitive P2X receptors. The density of innervation of dorsal horn neurones by primary afferent fibres increases during the postnatal development, particularly between P10 and P21 in the case of C-fibre inputs (Fitzgerald & Jennings, 1999). Therefore, it could be suggested that $\alpha\beta$-me-ATP activates P2X3 receptors on the primary afferent terminals to release glutamate and neuropeptides such as SP or CGRP. Such transmitters, through their metabotropic receptors, would eventually act on glycinergic nerve terminals to increase the probability of glycine release. However, in another set of experiments to elucidate such a possibility, t-ACPD (mGluR agonist), SP and CGRP had no effect on mIPSC frequency (data not shown). Additionally, the present results using thapsigargin (Fig. 7) also partly support the absence of a relationship with any metabotropic receptors.

P2X2, P2X4 and P2X6, particularly P2X4 and P2X6 subunit RNAs closely overlap in the dorsal horn of the spinal cord as well as the brain of adult rat. In addition, $[^3H]\alpha\beta$-me-ATP binding sites are widely distributed in the rat CNS and are closely correlated with *in situ* hybridization data on P2X4 and P2X6 mRNA distributions (Bo & Burnstock, 1994; Collo *et al.* 1996). Such findings suggest the possibility that these subunits can coassemble into heteromeric P2X receptors (Collo *et al.* 1996; Le *et al.* 1998*b*). In fact, when coexpressed, heteromeric P2X4/6 receptors have unique properties, such as increased sensitivities to $\alpha\beta$-me-ATP, 2MeS-ATP, suramin and PPADS, as compared with homomeric P2X4 or P2X6 receptors (Le *et al.* 1998*a*). These pharmacological profiles of P2X4/6 receptors are also consistent with the present findings, although it was not determined whether P2X4/6 receptors are sensitive to nanomolar TNP-ATP. In addition, RB-2, which potentiates P2X4 receptor-mediated currents but antagonizes P2X4/6 receptor-mediated currents, significantly blocked $\alpha\beta$-me-ATP-elicited presynaptic responses. Therefore, the most plausible conclusion is that heteromeric P2X4/6 receptors might be expressed in the spinal dorsal horn and are responsible for the $\alpha\beta$-me-ATP-elicited facilitation of spontaneous glycinergic transmission. Such a conclusion is consistent with recent findings suggesting that P2X4/6 receptors play a significant role in the regulation of excitatory transmitter release in central synapses (Le *et al.* 1998*a*; Kato & Shigetomi, 2001).

Effect of $\alpha\beta$-me-ATP on glycinergic eIPSCs

Our observation that $\alpha\beta$-me-ATP concentration-dependently inhibits glycinergic eIPSCs in P28–30 neurones is rather unexpected, as P2X receptors are normally Ca^{2+} permeable. Indeed, P2X2 receptors have been suggested to potentiate GABAergic eIPSCs in cultured dorsal horn neurones (Hugel & Schlichter, 2000). One possibility which would explain the present finding is

that $\alpha\beta$-me-ATP also acts postsynaptically to affect glycinergic eIPSC amplitude. However, this was not the case because the cumulative distribution in the amplitude of spontaneous events was not changed during the application of $\alpha\beta$-me-ATP. Alternatively, $\alpha\beta$-me-ATP might greatly depolarize the glycinergic nerve terminals and block the invasion of action potentials. Indeed, a recent study performed on rat hippocampus suggested that kainate, via ionotropic kainate receptors, inhibits evoked glutamate release by inactivation of Na^+ channels secondary to depolarization (Schmitz *et al.* 2000). Further studies are needed to determine the mechanism of the present P2X receptor-mediated presynaptic inhibition.

Physiological significance of $\alpha\beta$-me-ATP-sensitive P2X receptors

P2X receptors, especially P2X2 and P2X3, play an important role in the transduction of pain signalling within the dorsal horn area as well as the nerve terminals of primary afferent neurones (Kennedy & Leff, 1995; Burnstock & Wood, 1996; Cook *et al.* 1997). Surprisingly, P2X3 receptors have only been found in sensory neurones including trigeminal, dorsal root, nodose ganglia and their central terminals (Collo *et al.* 1996; Vulchanova *et al.* 1996, 1997). This suggests that P2X3 receptors mainly participate in the modulation of neurotransmitter release from the primary afferent fibres as well as in the transduction of pain signals in the peripheral sensory neurones. On the other hand, P2X2 receptors are likely to act as negative feedback modulator in the inhibitory presynaptic nerve terminals of the dorsal horn neurones (Hugel & Schlichter, 2000; Rhee *et al.* 2000). Our present results strongly suggest that $\alpha\beta$-me-ATP-sensitive P2X receptors can modulate neurotransmitter release from the glycinergic inhibitory presynaptic terminals of the adult spinal cord neurones.

In general, receptors responsible for fast synaptic transmission, such as AMPA, NMDA, GABA$_A$ and glycine receptors, reduce their decay time constants by switching their receptor subunits during postnatal development (Singer *et al.* 1998; Bellingham *et al.* 1998; Hutcheon *et al.* 2000). This suggests a functional role for synaptic transmission in the promotion of precise timing operations in the nervous system. Our results also present an example of a change in the presynaptic nerve terminals, that is, from non-desensitizing P2X2 receptors to moderately desensitizing $\alpha\beta$-me-ATP-sensitive P2X receptors during postnatal development. Therefore, the developmental changes in P2X receptors in the presynaptic nerve terminals may contribute to synaptic plasticity such as the regulation of neuronal excitability and the fine controlling of pain signals in the spinal cord dorsal horn neurones.

AKAIKE, N. & HARATA, N. (1994). Nystatin perforated patch recording and its application to analysis of intracellular mechanism. *Japanese Journal of Physiology* **44**, 433–473.

BARDONI, R., GOLDSTEIN, P. A., LEE, C. J., GU, J. G. & MACDERMOTT, A. B. (1997). ATP P2X receptors mediate fast synaptic transmission in the dorsal horn of the rat spinal cord. *Journal of Neuroscience* **17**, 5297–5304.

BELLINGHAM, M. C., LIM, R. & WALMSLEY, B. (1998). Developmental changes in EPCS quantal size and quantal content at a central glutamatergic synapse in rat. *Journal of Physiology* **511**, 861–869.

BO, X. & BURNSTOCK, G. (1994). Distribution of [^{3}H]α,β-methylene ATP binding sites in rat brain and spinal cord. *NeuroReport* **5**, 1601–1604.

BUELL, G., LEWIS, C., COLLO, G., NORTH, R. A. & SURPRENANT, A. (1996). An antagonist-insensitive P2X receptor expressed in epithelia and brain. *EMBO Journal* **15**, 55–62.

BURNSTOCK, G. & WOOD, J. N. (1996). Purinergic receptors: their role in nociception and primary afferent neurotransmission. *Current Opinion in Neurobiology* **6**, 526–532.

CHEN, C. C., AKOPIAN, A. N., SIVILOTTI, L., COLQUHOUN, D., BURNSTOCK, G. & WOOD, J. N. (1995). A P2X purinoceptor expressed by a subset of sensory neurons. *Nature* **377**, 428–431.

COLLO, G., NORTH, R. A., KAWASHIMA, E., MERLO-PICH, E., NEIDHART, S., SURPRENANT, A. & BUELL, G. (1996). Cloning of P2X5 and P2X6 receptors and the distribution and properties of an extended family of ATP-gated ion channels. *Journal of Neuroscience* **16**, 2495–2507.

COOK, S. P., VULCHANOVA, L., HARGREAVES, K. M., ELDE, R. & McCLESKEY, E. W. (1997). Distinct P2X receptors mediate ATP actions on nociceptive and non-nociceptive neurons. *Nature* **387**, 505–508.

DUNWIDDIE, T. V., DIAO, L. & PROCTOR, W. R. (1997). Adenine nucleotides undergo rapid, quantitative conversion to adenosine in the extracellular space in rat hippocampus. *Journal of Neuroscience* **17**, 7673–7682.

EDWARDS, F. A., GIBB, A. J. & COLQUHOUN, D. (1992). ATP receptor-mediated synaptic currents in the central nervous system. *Nature* **359**, 144–147.

EVANS, R. J., DERKACH, V. & SURPRENANT, A. (1992). ATP mediates fast synaptic transmission in mammalian neurons. *Nature* **357**, 503–505.

FITZGERALD, M. & JENNINGS, E. (1999). The postnatal development of spinal sensory processing. *Proceedings of the National Academy of Sciences of the USA* **96**, 7719–7722.

GALLIGAN, J. J. & BERTRAND, P. P. (1994). ATP mediates fast synaptic potentials in enteric neurons. *Journal of Neuroscience* **12**, 7563–7571.

GARCIA-GUZMAN, M., SOTO, F., GOMEZ-HERNANDEZ, J. M., LUND, P. E. & STUHMER, W. (1997). Characterization of recombinant human P2X4 receptor reveals pharmacological differences to the rat homologue. *Molecular Pharmacology* **51**, 109–118.

GU, J. G. & MACDERMOTT, A. B. (1997). Activation of ATP P2X receptors elicits glutamate release from sensory neuron synapses. *Nature* **389**, 749–753.

HUGEL, S. & SCHLICHTER, R. (2000). Presynaptic P2X receptors facilitate inhibitory GABAergic transmission between cultured rat spinal cord dorsal horn neurons. *Journal of Neuroscience* **20**, 2121–2130.

HUTCHEON, B., MORLEY, P. & POULTER, M. O. (2000). Developmental change in GABA$_A$ receptor desensitization kinetics and its role in synapse function in rat cortical neurons. *Journal of Physiology* **522**, 3–17.

KATO, F. & SHIGETOMI, E. (2001). Distinct modulation of evoked and spontaneous EPSCs by purinoceptors in the nucleus tractus solitarii of the rat. *Journal of Physiology* **530**, 469–486.

KENNEDY, C. & LEFF, P. (1995). Painful connection for ATP. *Nature* **377**, 385–386.

KHAKH, B. S., BURNSTOCK, G., KENNEDY, C., KING, B. F., NORTH, R. A., SEGUELA, P., VOIGT, M. & HUMPHREY, P. P. A. (2001). International union of pharmacology. XXIV. Current status of the nomenculature and properties of P2X receptors and their subunits. *Pharmacological Reviews* **53**, 107–118.

KHAKH, B. S., PROCTOR, W. R., DUNWIDDIE, T. V., LABARCA, C. & LESTER, H. A. (1999). Allosteric control of gating and kinetics at P2X4 receptor channels. *Journal of Neuroscience* **19**, 7289–7299.

LE, K.-T., BABINSKI, K. & SEGUELA, P. (1998a). Central P2X4 and P2X6 channel subunits coassemble into a novel heteromeric ATP receptor. *Journal of Neuroscience* **18**, 7152–7159.

LE, K.-T., VILLENEUVE, P., RAMJAUN, A. R., MAPHERSON, P. S., BEAUDET, A. & SEGUELA, P. (1998b). Sensory presynaptic and widespread somatodendritic immunolocalization of central ionotropic P2X ATP receptor. *Neuroscience* **83**, 177–190.

LEWIS, C., NEIDHART, S., HOLY, C., NORTH, R. A., BUELL, G. & SURPRENANT, A. (1995). Coexpression of P2X2 and P2X3 receptor subunits can account for ATP-gated currents in sensory neurons. *Nature* **377**, 432–435.

LI, P., CALEJESAN, A. A. & ZHUO, M. (1998). ATP P2X receptors and sensory synaptic transmission between primary afferent fibers and spinal dorsal horn neurons in rats. *Journal of Neurophysiology* **80**, 3356–3360.

LI, Y.-Q., LI, H., KANEKO, T. & MIZUNO, N. (1999). Local circuit neurons showing calbindin D28K-immunoreactivity in the substantia gelatinosa of the medullary dorsal horn of the rat. An immunohistochemical study combined with intracellular staining in slice preparation. *Brain Research* **840**, 179–183.

NORTH, R. A. & BARNARD, E. A. (1997). Nucleotide receptors. *Current Opinion in Neurobiology* **7**, 346–357.

RHEE, J. S., ISHIBASHI, H. & AKAIKE, N. (1999). Calcium channels in the GABAergic presynaptic nerve terminals projecting to Meynert neurons of the rat. *Journal of Neurochemistry* **72**, 800–807.

RHEE, J. S., WANG, Z. M., NABEKURA, J., INOUE, K. & AKAIKE, N. (2000). ATP facilitates spontaneous glycinergic IPSC frequency at dissociated rat dorsal horn interneuron synapses. *Journal of Physiology* **524**, 471–483.

SALTER, M. W. & HICKS, J. L. (1995). ATP causes release of intracellular Ca^{2+} via the phospholipase C beta/IP$_3$ pathway in astrocytes from the dorsal spinal cord. *Journal of Neuroscience* **15**, 2961–2971.

SCHMITZ, D., FRERKING, M. & NICOLL, R. A. (2000). Synaptic activation of presynaptic kainate receptors on hippocampal mossy fiber synapses. *Neuron* **27**, 327–338.

SINGER, J. H., TALLEY, E. M., BAYLISS, D. A. & BERGER, A. J. (1998). Development of glycinergic transmission to rat brain stem motoneurons. *Journal of Neurophysiology* **80**, 2608–2620

TASCHENBERGER, H., JUTTNER, R. & GRANTYN, R. (1999). Ca^{2+}-permeable P2X receptor channels in cultured rat retinal ganglion cells. *Journal of Neuroscience* **19**, 3353–3366.

TODD, A. J. (1988). Electron microscope study of Golgi-stained cells in lamina II of the rat spinal dorsal horn. *Journal of Comparative Neurology* **275**, 145–157.

TORRES, G. E., EGAN, T. M. & VOIGT, M. M. (1999). Hetero-oligomeric assembly of P2X receptor subunits. Specificities exist with regard to possible parters. *Journal of Biological Chemistry* **274**, 6653–6659.

TORRES, G. E., HAINES, W. R., EGAN, T. M. & VOIGT, M. M. (1998). Co-expression of P2X1 and P2X5 receptor subunits reveals a novel ATP-gated ion channel. *Molecular Pharmacology* **54**, 989–993.

VALERA, S., HUSSY, N., EVANS, R. J., ADAMI, N., SURPRENANT, A. & BUELL, G. (1994). A new class of ligand-gated ion channel defined by P2X receptor for extracellular ATP. *Nature* **371**, 516–519.

VIRGINIO, C., ROBERTSON, G., SURPRENANT, A. & NORTH, R. A. (1998). Trinitrophenyl-substituted nucleotides are potent antagonists selective for P2X1, P2X3 and heteromeric P2X2/3 receptors. *Molecular Pharmacology* **53**, 969–973.

VULCHANOVA, L., ARVIDSSON, U., RIEDL, M., WANG, J., BUELL, G., SURPRENANT, A., NORTH, R. A. & ELDE, R. (1996). Differential distribution of two ATP-gated channels (P2X receptors) determined by immunocytochemistry. *Proceedings of the National Academy of Sciences of the USA* **93**, 8063–8067.

VULCHANOVA, L., RIEDL, M. S., SHUSTER, S. J., BUELL, G., SURPRENANT, A., NORTH, R. A. & ELDE, R. (1997). Immunohistochemical study of the P2X2 and P2X3 receptor subunits in rat and monkey sensory neurons and their central terminals. *Neuropharmacology* **36**, 1229–1242.

VULCHANOVA, L., RIEDL, M. S., SHUSTER, S. J., STONE, L. S., HARGREAVES, K. M., BUELL, G., SURPRENANT, A., NORTH, R. A. & ELDE, R. (1998). P2X3 is expressed by DRG neurons that terminate in inner lamina II. *European Journal of Neuroscience* **11**, 3470–3478.

Corresponding author

N. Akaike: Department of Cellular and System Physiology, Graduate School of Medical Sciences, Kyushu University, Maidashi 3-1-1, Fukuoka 812-8582, Japan.

Email: akaike@physiol2.med.kyushu-u.ac.jp